

Article

Application of Anticoincidence Technology to Burn-Up Measurement Systems in High-Temperature Gas-Cooled Reactors

Cui Mao ^{1,2,3,4}, Yi-Bao Liu ⁴ and Li-Guo Zhang ^{1,2,3,*}

¹ Institute of Nuclear and New Energy Technology, Tsinghua University, Beijing 10084, China; 18110023112@163.com

² Key Laboratory of Advanced Reactor Engineering and Safety, Ministry of Education, Beijing 10084, China

³ Advanced Nuclear Energy Technology Collaborative Innovation Center, Beijing 10084, China

⁴ Institute of Nuclear Science and Engineering, East China University of Technology, Nanchang 330000, China; liuyb01@mails.tsinghua.edu.cn

* Correspondence: lgzhang@tsinghua.edu.cn; Tel.: +86-10-6279-2767

Received: 30 June 2018; Accepted: 11 August 2018; Published: 14 August 2018



Abstract: Nuclear energy is the focus of sustainable energy development worldwide. A high-temperature gas-cooled reactor (HTGR) plays a vital role in the development of nuclear energy. In a pebble-bed HTGR, the burn-up measurement system is important for ensuring reactor safety and economy. This study optimized a burn-up measurement system by adding anticoincidence technology with bismuth germanium oxide (BGO) crystals and a plastic scintillator used as anticoincidence detectors. Through Monte Carlo simulation, the detection effects of two different anticoincidence detectors on fuel elements were compared and analyzed. The study focused on varying the wall thickness and top thickness of these detectors to optimize the peak-to-Compton ratio (P/C). The results showed that the size of the BGO detector with the best anticoincidence effect (P/C of 727) consists in a diameter of 140 mm and a length of 210 mm. The best plastic scintillator size (P/C of 180) consists in a diameter of 260 mm and a length of 260 mm. Adding the anticoincidence technology lowered the Compton plateau of the measured gamma spectrum and significantly improved the detection performance of the burn-up measurement system. The new burn-up measurement system has improved detection precision not only for Cs-137 but also for low-activity nuclides.

Keywords: high-temperature gas-cooled reactor; burn-up measurement; anti-coincidence technology; peak to Compton ratio; nuclear energy

1. Introduction

With the development of society and economy, the shortage of energy is becoming more and more serious. Therefore, the sustainable development of energy has become the focus of much of the world. An efficient, clean, and economic energy, nuclear energy plays an important role in the field of sustainable energy [1], and the high-temperature gas-cooled reactor (HTGR) is one of the preferred reactors for the fourth generation nuclear power systems in the current international nuclear energy field [2]. China has been working on HTGRs since the 1970s [3]. The Institute of Nuclear and New Energy Technology of Tsinghua University built a 10 MW pebble-bed high-temperature gas-cooled experimental reactor (HTR-10). This study is mainly based on the HTR-10, which is still operated by this university.

The HTGR has the characteristics of non-stop refueling and fuel element recycling [4,5]. The burn-up measurement system of the reactor uses a high-purity germanium (HPGe) detector for nondestructive on-line measurement of fuel element burnup. The result of the measurement

determines the disposition of the fuel element, that is, to unload it as spent fuel or return it to the core [6]. If the measured burnup is incorrect, and spent fuel is recycled back into the core, the fuel cladding material can be damaged and increase the risk of radioactive material leakage [7–10]. In contrast, if the fuel has not yet reached the discharge burnup value, and it is discharged as spent fuel, this leads to increased cost and nuclear fuel waste [11]. Thus, the accuracy of burnup measurement is very important for the safety and economy of an HTGR.

To improve the accuracy and precision of the HTGR burnup measurement system, scholars all over the world have been carried out a large amount of researches. These researches are mainly on the geometric structure of the collimator, the deviation from the center of the fuel element, the attenuation factor of the measurement system, the detection limit of the detector and the shielding efficiency, and the effect of fuel element cooling time on the burnup [12,13]. However, there is currently no research on the application of anticoincidence technology to burnup measurement.

The HTR-10 in China uses a burnup measurement system based on an HPGe detector to measure γ -ray activity from Cs-137 [14]. However, the HTR-10 has intermittent operation, short operation times, and long shutdown periods; the burnup of two fuel elements with the same activity may be different. This leads to difficulties in calculating the burnup of the fuel elements by measuring only the activity of Cs-137. It is necessary to measure additional radionuclides to improve the burnup measurement results. To solve this problem, this study proposes to add anti-coincidence measurement technology to the original burnup measurement system. The technology uses a common bismuth germanium oxide (BGO) crystal and plastic scintillator as an anticoincidence detector to reduce the Compton plateau of the γ -ray spectrum [15–17]. This can make the measurement of some low-activity nuclides possible and at the same time improve the accuracy of Cs-137 detection. The design was developed through Monte Carlo simulation [18,19], which provided an important theoretical reference for the construction of the new burnup measurement system.

2. Materials and Methods

The burnup measurement system has five main parts: elevator, collimator, sealing flange, lead chamber, and HPGe detector (Figure 1) [20]. Measurement begins after the fuel element is raised to the elevator. After being attenuated by the elevator pipe and sealing flange, the γ -rays pass through the collimator to the HPGe probe. The counts captured by the probe are analyzed for the gamma spectrum using GammaVision and Genie-2000 spectroscopy software to obtain the required nuclide information, which determines the burnup online. Fuel element with burnup greater than the burnup limit is discharged as spent fuel, and fuel with burnup less than the burnup limit is recycled back into the core.

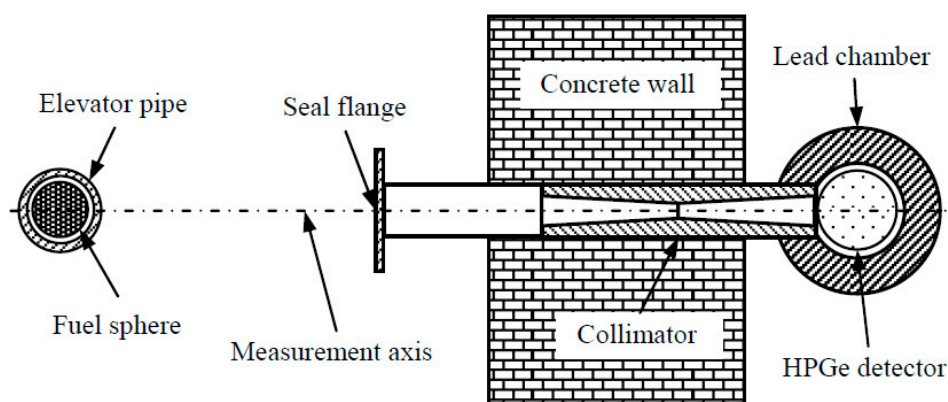


Figure 1. Schematic diagram of the burnup measurement system of HTR-10.

The original burnup measurement method was to calculate the burnup by measuring the activity of Cs-137 in the fuel element, because there is a one-to-one correspondence between the activity of Cs-137 and the fuel element burnup, as shown in Equation (1) [21].

$$BU = \frac{10^6 E_f}{G_b Y_7 \lambda_7} e^{\lambda_7(t-t^*)} A_7 \quad (1)$$

where A_7 is the activity of Cs-137, λ_7 and Y_7 are decay constant of Cs-137 and fission yield, G_b is the mass of heavy metal (unit: g), and E_f is U-235 in one fission to release the energy of 197 MeV. t is measuring time, and t^* is a media time.

As discussed in the previous section, intermittent operation of HTR-10 means that the radioactive nuclides (including Cs-137) in some fuel spheres decay during long shutdown periods. This reduces the activity of the nuclide but does not change the burnup of the fuel. (These problems will also exist for the larger HTR-PM modules currently under construction.) This leads to a situation where two elements can show the same activity at the time of burnup measurement but have an actual burnup that is different, causing inaccurate results for judging burnup. To solve this problem, we need to understand the history of fuel element burnup, which tells us how many cycles the fuel elements have experienced and the specific burnup process during operation. To understand the burnup history of fuel elements, it is necessary to measure other nuclides, such as Co-60, in the fuel for supplementary analysis.

The anticoincidence measurement system developed in this study consists of a main detector and an annular detector. During measurement, the γ -rays emitted by radionuclides hit the HPGe detector to generate pulse signals, and the scattered photons escaping from the main detector will enter the peripheral anticoincidence detector and generate anticoincidence pulses. If both the primary detector and the anticoincidence detector output a signal at the same time, the signal pulse is not recorded. The signal pulse is recorded only when the main detector has outputs. In this way, because the signals generated by escaping photons, such as Compton photons, are not recorded, the Compton plateau is greatly reduced by anticoincidence, which improves the nuclide measurement accuracy. The working principle of the system's anticoincidence measurement process is shown in Figure 2.

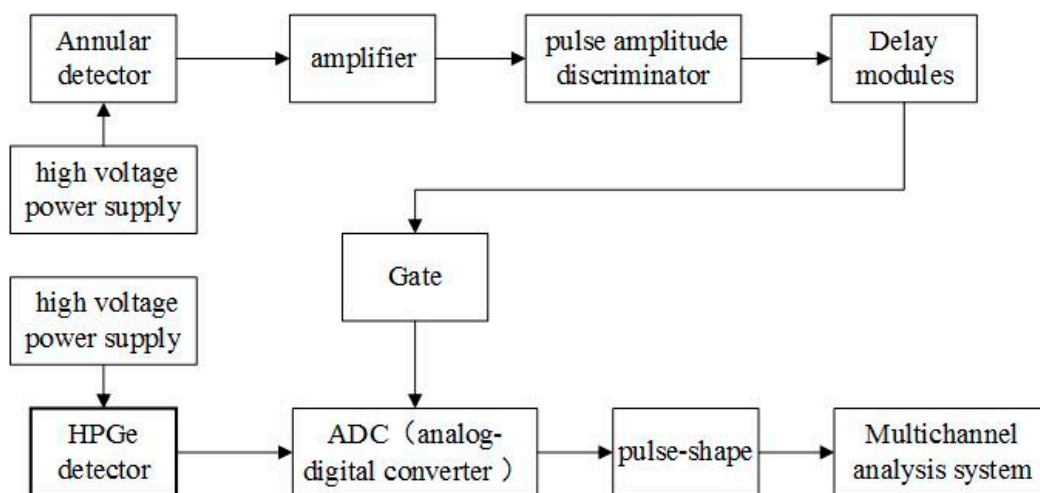


Figure 2. Schematic of anticoincidence circuit in the HPGe detector.

3. Results

3.1. Model Calculation and Parameters

Geant4 is a detector simulation toolkit written in the C++ language [22]. It uses the Monte Carlo program to simulate the physical process of high-energy particle transportation in the detector. It can construct a complex geometric structure of the detector, establish the physical process model of the interesting particles, trace the particles, and display the particle tracks. It has a powerful spatial modeling ability.

In this paper, the operating system of simulation was Debian GNU/Linux 3.16, and the HTR-10 burnup measurement system model was constructed with 9.6.p03 version of Geant4 [23,24]. The energy deposition data of the rays in the detector were collected and counted to form the results reflecting the performance of the detector. The number of simulated particles in each group was 300,000 and the calculation time was 42 s.

The aim of this study was to determine the shape parameters of the annular detector by simulating the anticoincidence effect of the annular detector and the HPGe detector. The gamma spectra of fuel elements after core irradiation are very complicated. The presence of the collimator, elevator, and sealing flange degrades the calculation efficiency and precision of the Geant4 particle simulation software. Therefore, to simplify the calculation without changing the nature of the target phenomena, the exit direction of γ -rays was limited to a single direction, and the model was further simplified by splitting it into two parts for the two detectors [25]. Other ancillary structures located between the source and detectors in the burnup measurement system were ignored, because they can also degrade the calculation efficiency. Such structures included the flat head made of 16MnR steel, sealing materials, and grade Cr-45 steel.

In the model design, the anticoincidence detector was given a cup-shaped structure with cylindrical outer wall and cylindrical inner wall forming a hole with a diameter of 100 mm and a height of 200 mm along the central axis. The HPGe probe was placed in this hole. A circular hole with a diameter of 10 mm pierced the side wall of the anticoincidence. The axis of this hole was coincident with the axis of the collimator, which was used to collect γ -rays. The annular detector used BGO crystal and plastic scintillator. Note that the plastic scintillator had a low detection efficiency for γ -rays and is used only for preliminary experimental testing.

The P-type HPGe detector used in the main detector had an energy resolution (full-width at half maximum) of 1.85 keV for a 1332 keV γ -ray from Co-60 and relative efficiency of 30%. The aluminum shell (end window) diameter was 76 mm, the end window top and side wall thicknesses were 1 mm, and the distance between the top of the probe crystal and the aluminum protective shell was 4 mm. The side wall thickness of the aluminum cup was 0.8 mm, the probe crystal end was 62.6 mm in diameter, the crystal annular thickness was 25.9 mm, and the center (electrode) hole of the probe crystal was 0.8 mm. A simplified model of the anticoincidence measurement system is shown in Figure 3.

In conformance with the IEEE [26] γ -ray detector measurement standard, this study used 1332 keV γ -rays from Co-60 in the fuel element for single-peak simulation. Its peak-to-Compton ratio (P/C) (see Equation (2)) was used as a reference to analyze the anticoincidence measurement effect of system. Geant4 software was used to simulate the anticoincidence effect between annular detectors of different sizes and the HPGe detector to determine the geometric dimensions for an optimum P/C.

$$P/C = N_P/N_C \quad (2)$$

where N_P is the number of counts in the peak channel, and N_C is average number of counts per channel between 1040 and 1096 keV of the Compton spectrum.

3.2. Analysis Results of Two Detectors

There are two main factors influencing the detection efficiency of the annular detector: material and geometric structure. Since the materials, BGO crystal and plastic scintillator, have been determined, this study mainly analyzed the effect of specific geometric parameters on the anticoincidence between the main detector and the two annular detectors. Two main geometric parameters, wall thickness and top thickness, as shown in Figure 4, were varied. The other dimensions were as given in Section 3.1.

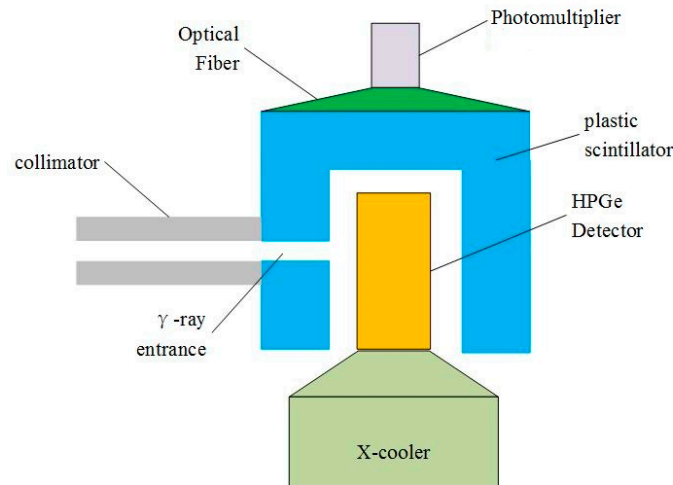


Figure 3. Simplified model of anticoincidence measurement system.

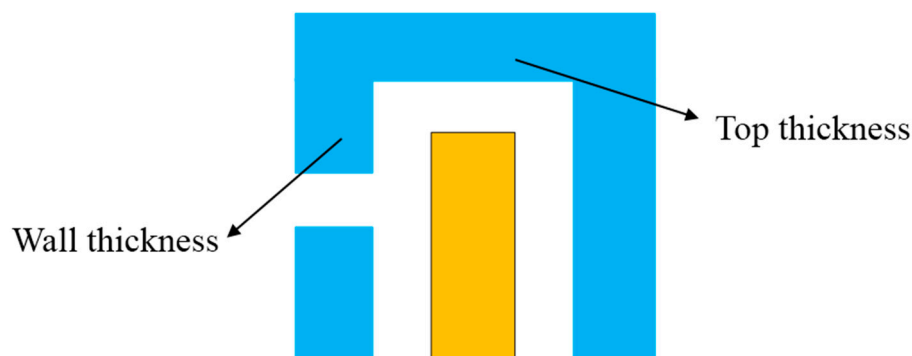


Figure 4. Two main geometric parameters of the annular detector.

3.2.1. Plastic Scintillator Detector Anticoincidence Effect Analysis

The initialize size of the plastic scintillator detector was set to a diameter of 200 mm and length of 260 mm, and the initial wall thickness was set to 50 mm. The scintillator was composed of matrix scintillation materials and wavelength shifting fiber with a density of 1.05 g/cm^3 . First, the wall thickness was increased from 50 to 100 mm in 10 mm increments, while the top thickness of the annular detector remained unchanged from its initial value of 60 mm. The P/C was determined for each wall thickness, and the results are shown in Table 1 and Figure 5.

As can be seen from Figure 5, as the detector wall thickness increased, the P/C had an obvious rising trend and increased by a total of 70. The average P/C growth of the system was 14 per 10 mm increment. When the wall thickness increased to 80 mm, the growth of P/C slowed down. According to the comprehensive consideration of the P/C effect, material cost, and system geometry space, a wall thickness of 80 mm was determined to be optimal.

Using the selected wall thickness of 80 mm, to make the results more representative, the anticoincidence effect simulation was repeated, while the top thickness was varied from 50 to 90 mm in 10 mm increments (not from the initial value of 60 mm). The simulation results are shown in Table 2 and Figure 5.

Table 1. P/C of the system with increasing scintillator wall thickness.

Wall Thickness/mm	P/C of Plastic Scintillator				
	Peak Channel	Np	Total Counts from 1040 keV to 1096 keV	Nc	P/C
50	6774	13,284	27,209	95	139
60	6774	13,189	24,364	85	154
70	6774	13,241	22,321	78	169
80	6774	13,174	20,755	73	180
90	6774	13,238	19,241	67	196
100	6774	13,146	17,926	63	209

Table 2. P/C of the system with increasing top thickness and an 80 mm wall thickness in the scintillator.

Top Thickness/mm	P/C of Plastic Scintillator				
	Peak Channel	Np	Total Counts from 1040 keV to 1096 keV	Nc	P/C
50	6774	13,122	21,214	74	176
60	6774	13,174	20,755	73	180
70	6774	13,094	19,924	70	187
80	6774	13,224	19,792	69	190
90	6774	13,191	19,397	68	194

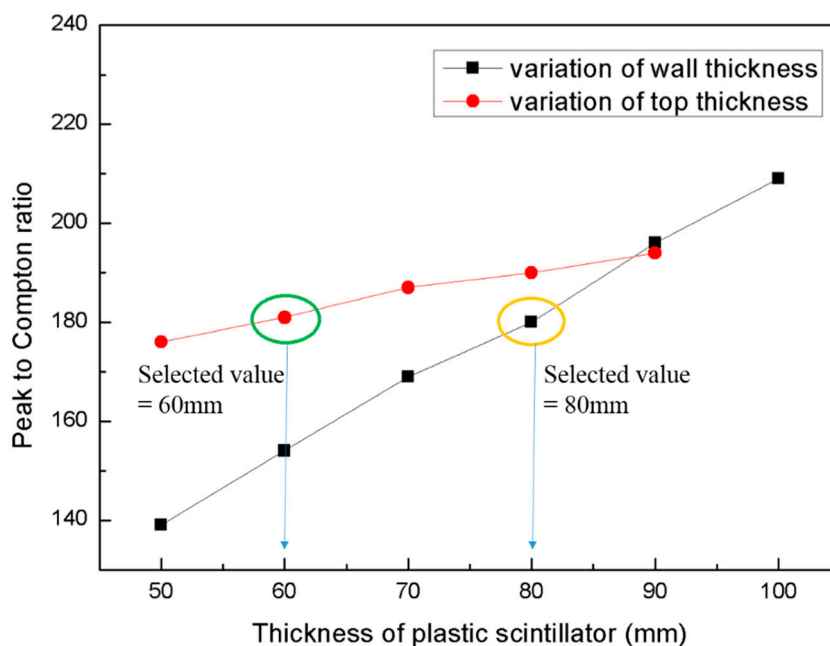


Figure 5. System P/C trend with increasing scintillator wall and top thickness.

As can be seen from Table 2, as the top thickness of the plastic scintillator detector increased, the P/C of the system presented an increasing trend. The P/C of the system increased by 18 overall, and the average increase was 4.5 per 10 mm increment. As can be seen from the growth curve in Figure 5, the overall P/C growth trend was relatively slow. This indicates that a changing top thickness

has less effect on the P/C of the system. Therefore, in terms of P/C effect and material cost, it is more appropriate to use the initial top thickness value of 60 mm.

3.2.2. BGO Detector Anticoincidence Effect Analysis

The size of the BGO detector was set to a diameter of 110 mm and length of 210 mm. The initial value of the top thickness was 10 mm, and the initial value of the wall thickness was 5 mm. BGO has a density of 7.13 g/cm^3 . Because the detection efficiency of the BGO detector is sensitive to its size, the thickness increment of this simulation was 5 mm.

In the first simulation, the top thickness of the annular detector was kept at its initial value of 10 mm while the wall thickness was varied from 5 to 20 mm to observe its effect on the anticoincidence of the system. The results are shown in Table 3 and Figure 6.

Table 3. P/C of the system with increasing bismuth germanium oxide (BGO) detector wall thickness.

Wall Thickness/mm	P/C of BGO Crystals				
	Peak Channel	Np	Total Counts from 1040 keV to 1096 keV	Nc	P/C
5	6774	13,129	11,962	42	313
10	6774	13,048	6535	23	569
15	6774	13,005	5472	19	677
20	6774	13,079	5129	18	727
25	6774	13,028	5071	18	732
30	6774	13,139	5145	18	728

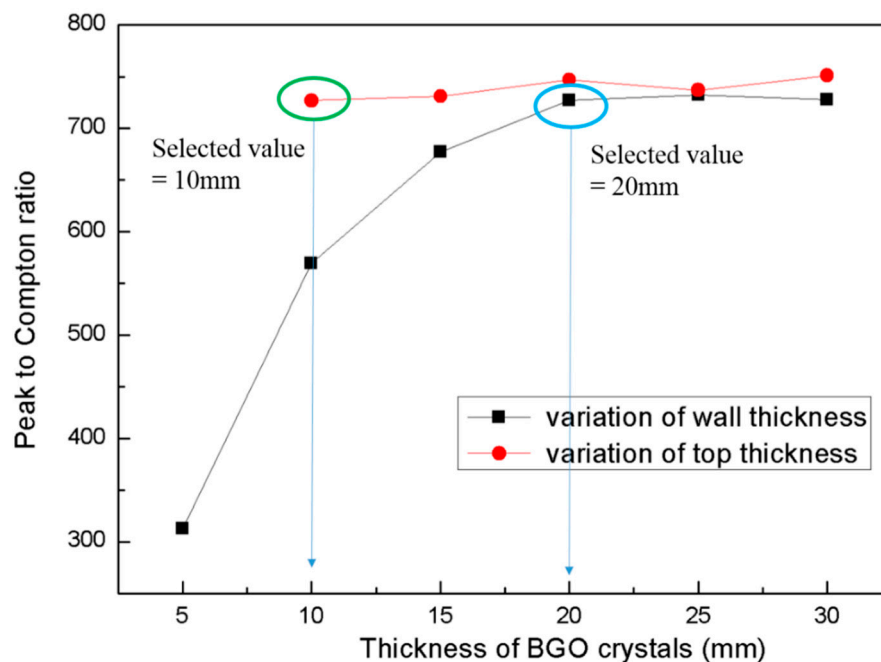


Figure 6. System P/C trend with increasing BGO wall and top thickness.

As can be seen from Figure 6, as the wall thickness of the BGO detector increased, the anti-coincidence effect of the system showed a significant upward trend. The P/C of the system increased from 313 to 727 in increments of 414. However, when the wall thickness reached 20 mm, the P/C trend flattened, with slow growth and stagnation at a value of around 730. Considering the above results, material cost, and geometric space of the system, a 20 mm wall thickness was deemed optimal.

Using the selected wall thickness of 20 mm, the anticoincidence effect simulation was repeated while the top thickness was varied from 10 to 30 mm, also in 5 mm increments. The simulation results are shown in Table 4 and Figure 6.

Table 4. P/C of the system with increasing top thickness and 20 mm wall thickness in the annular BGO detector.

Top Thickness/mm	P/C of BGO Crystals				
	Peak Channel	Np	Total Counts from 1040 keV to 1096 keV	Nc	P/C
10	6774	13,079	5129	18	727
15	6774	12,942	5047	18	731
20	6774	13,054	4980	17	747
25	6774	13,012	5033	18	737
30	6774	13,171	4996	18	751

As can be seen from the results, as the top thickness of the detector increased, the P/C changed less than it did in response to wall thickness changes. When the top thickness reached 30 mm, the P/C had only increased by 24, which produced a basically horizontal curve, as shown in Figure 6. This also indicates that changing the top thickness has less effect on the anticoincidence of the system. Considering the above results, the initial value of 10 mm was deemed optimal for the top thickness.

4. Discussion

The results in Section 3 determined the wall and top thickness parameters that optimized the P/C effects of the two annular detectors, with a diameter of 260 mm and a length of 260 mm for the scintillator and a diameter of 210 mm a length of 140 mm for the BGO detector. The P/C of the burnup measurement system was simulated without an anticoincidence detector. It was found that the P/C was around 69, as shown in Table 5. According to the data in Tables 4 and 5, after adding the BGO detector, the P/C of the system increased by 685. Figure 7 shows the anticoincidence effect diagram of the same spectrum with and without the annular BGO detector. As can be seen from the Figure 7, when the BGO detector was present, the Compton plateau for γ -rays was greatly reduced, and the peaks of the γ -ray spectrum were much more obvious, which shows that, after adding anticoincidence technology, detection performance of the burnup measurement system improved significantly.

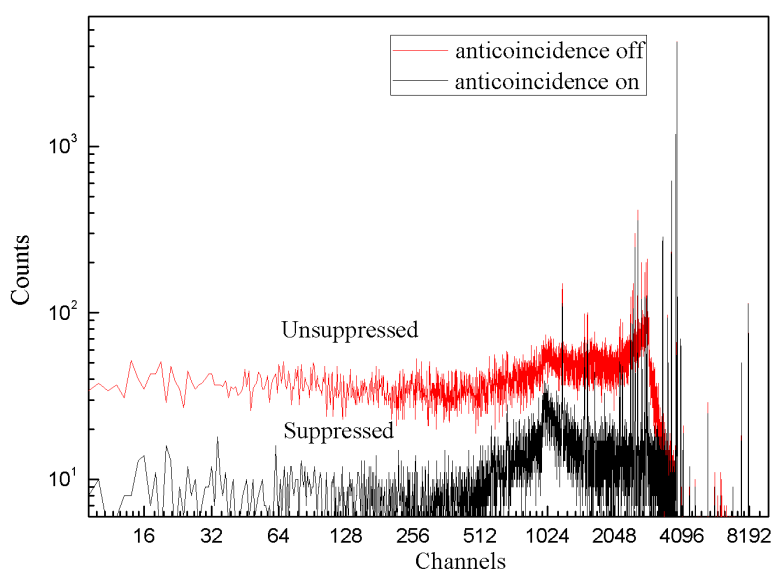


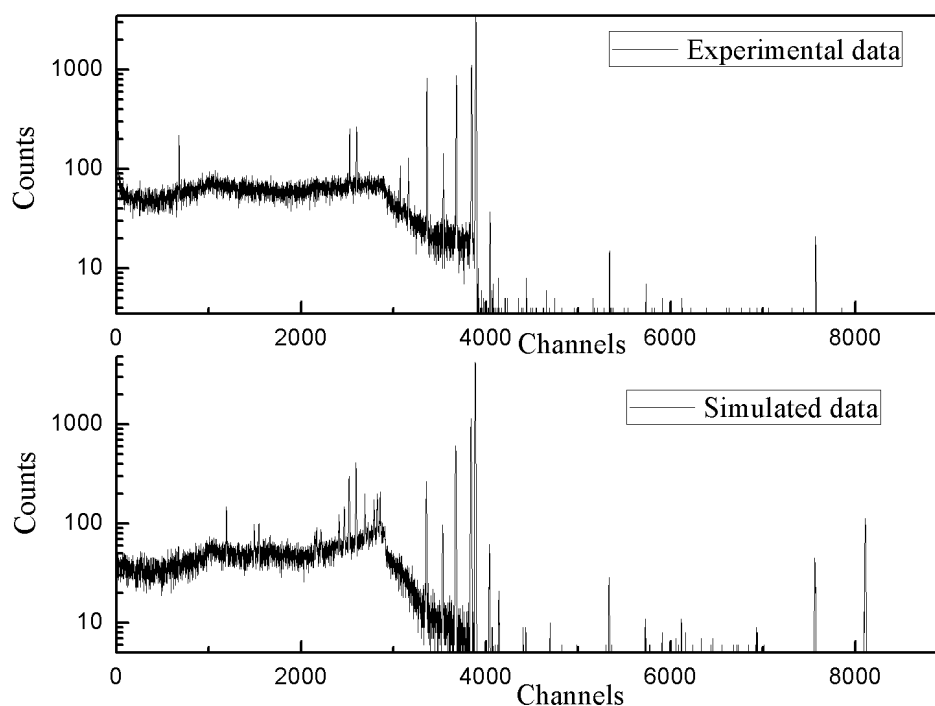
Figure 7. The anticoincidence effect diagram of the same spectrum with and without the BGO detector.

Table 5. P/C of the system with no anticoincidence detector.

Peak Channel	Np	Total Counts from 1040 keV to 1096 keV	Nc	P/C
6774	13,109	53,767	189	69
6774	13,039	53,685	188	69
6774	13,038	53,792	189	69

4.1. Comparative Analysis of Experimental Results and Simulation Results

To verify the reliability of the simulation, the simulated data and the data measured by the HTR-10 burnup measurement system were compared, as shown in Figure 8. As can be seen in the figure, the Compton plateau for counts of the two spectra is slightly different because the actual measurement is far more complex than the simulation. The actual measurement environment contains natural radionuclides and other radioactive materials, and the effects of these conditions cannot be accurately simulated by the Geant4 software. Additionally, the peaks in the simulated spectrum are in good agreement with the actual measured peaks of the energy spectrum, which also proves that all simulations performed in this study are accurate and reliable.

**Figure 8.** A contrast diagram of experimental data and simulated data.

4.2. Statistical Error Analysis of Simulated Data

The number of output pulses obtained from radiation measurement is a random variable that follows the Poisson distribution. Therefore, data measured under the same conditions may be completely different. As the simulation run-time approaches infinity, the arithmetic mean value of the experimental value will tend to the mathematical expectation, which is not possible in practice. In fact, we generally regard the arithmetic mean of finite time (usually once) as a real “mathematical expectation,” which leads to error. This error is called statistical error, and it is a special error in the measurement of radiation because of the statistical nature of radiation measurement. In this study, the peak area errors and the background count errors of Co-60 γ -rays were calculated using different shape parameters, and the results are shown in Table 6. From the data in Table 6, we can see that the

statistical error range of γ -rays for different geometries was between 0.53 and 1.40%. These errors are small, indicating again that the simulated data in this paper are accurate and reliable.

Table 6. Statistical error analysis.

Detector Type	Statistical Error/%	Wall Thickness/mm					
		50/5	60/10	70/15	80/20	90/25	100/30
Plastic scintillator	Np error	0.87	0.87	0.87	0.87	0.87	0.87
	Background error	0.61	0.64	0.67	0.69	0.72	0.75
BGO crystals	Np error	0.87	0.87	0.88	0.87	0.88	0.87
	Background error	0.91	1.24	1.35	1.40	1.40	1.39

5. Conclusions

This study evaluated the improvement of a burnup measurement system in an HTGR using BGO crystals and a plastic scintillator. The anticoincidence effect of two annular detectors with different geometric parameters was analyzed by Monte Carlo simulation, which provided an important theoretical basis for the optimization of the burnup measurement system. The following conclusions were obtained.

- (1) As the wall and top thickness of the two annular detectors increased, the P/C of the γ -rays showed an increasing trend to varying degrees. The influence of wall thickness increases on the P/C of the system was found to be greater than that of increases in the top thickness.
- (2) When the wall thickness of the plastic scintillator increased from the value of 50 to 100 mm, the P/C of the system increased by 70. For every 10 mm increase in wall thickness, the mean increase of the P/C of the system was 14. After the wall thickness increased to 80 mm, the growth trend of P/C gradually leveled off. The geometric size producing the best anticoincidence effect was estimated to consist in a diameter of 260 mm and a length of 260 mm, and its P/C is 180.
- (3) In the detector using BGO crystals, when the wall thickness increased from 5 to 20 mm, the system showed an obvious rising trend, with the P/C increasing by a total of 414. However, after the wall thickness reached 20 mm, the P/C growth curve flattened out, with a peak of around 730. Taking into account the system's anticoincidence effect, geometric space, material cost, and other factors, we determined the best anticoincidence BGO crystal geometry for a detector size of a diameter of 140 mm and a length of 210 mm, and it achieved a P/C of 727.

This study is of great importance to the safety and economy of HTGRs and the sustainable development of nuclear energy.

Author Contributions: C.M. performed all of the experiments, analyzed the data, and wrote the manuscript, L.-G.Z. and Y.-B.L. were the principle investigator and supervised all work.

Funding: The research was jointly supported by the Nuclear Development Project and the National Major Science and Technology Project (Grant No. ZX06901).

Conflicts of Interest: The authors declare no conflicts of interest.

References

1. Verfondern, K.; Lensa, W.V. Past and present research in Europe on the production of nuclear hydrogen with HTGR. *Prog. Nucl. Energy* **2005**, *47*, 472–483. [[CrossRef](#)]
2. International Atomic Energy Agency. *Current Status and Future Development of Modular High Temperature Gas Cooled Reactor Technology*; IAEA-TECDOC-1198; International Atomic Energy Agency: Vienna, Austria, 2001.
3. Zhang, Z.; Yu, S. Future HTGR developments in China after the criticality of the HTR-10. *Nucl. Eng. Des.* **2002**, *218*, 249–257. [[CrossRef](#)]

4. Kuijper, J.C.; Raepsaet, X.; De Haas, J.B.M.; Von Lensa, W.; Ohlig, U.; Ruetten, H.J.; Brockmann, H.; Damian, F.; Dolci, F.; Bernnat, W.; et al. HTGR reactor physics and fuel cycle studies. *Nucl. Eng. Des.* **2006**, *236*, 615–634. [[CrossRef](#)]
5. Chersola, D.; Lomonaco, G.; Marotta, R. The VHTR and GFR and their use in innovative symbiotic fuel cycles. *Prog. Nucl. Energy* **2015**, *83*, 443–459. [[CrossRef](#)]
6. Yan, W.H.; Zhang, L.G.; Zhang, Z.; Zhang, Y.; Xiao, Z.G. Prototype studies on the nondestructive online burnup determination for the modular pebble bed reactors. *Nucl. Eng. Des.* **2014**, *267*, 172–179. [[CrossRef](#)]
7. Sawa, K.; Minato, K. An Investigation of Irradiation Performance of High Burnup HTGR Fuel. *J. Nucl. Sci. Technol.* **1999**, *36*, 781–791. [[CrossRef](#)]
8. Ueta, S.; Aihara, J.; Sawa, K.; Yasuda, A.; Honda, M.; Furihata, N. Development of high temperature gas-cooled reactor (HTGR) fuel in Japan. *Prog. Nucl. Energy* **2011**, *53*, 788–793. [[CrossRef](#)]
9. Sawa, K.; Ueta, S. Research and development on HTGR fuel in the HTRR project. *Nucl. Eng. Des.* **2004**, *233*, 163–172. [[CrossRef](#)]
10. Lee, Y.W.; Park, J.Y.; Kim, Y.K.; Lee, Y.W.; Park, J.Y.; Kim, Y.K.; Jeong, K.C.; Kim, W.K.; Kim, B.G.; Kim, Y.M.; et al. Development of HTGR-coated particle fuel technology in Korea. *Nucl. Eng. Des.* **2008**, *238*, 2842–2853. [[CrossRef](#)]
11. Tang, C.; Tang, Y.; Zhu, J.; Zou, Y.; Li, J.; Ni, X. Design and manufacture of the fuel element for the 10 MW high temperature gas-cooled reactor. *Nucl. Eng. Des.* **2002**, *218*, 91–102. [[CrossRef](#)]
12. Wei-Hua, Y.; Li-Guo, Z.; Yan, Z.; Zhao, Z.; Zhi-Gang, X. Monte Carlo studies on the burnup measurement for the high temperature gas cooling reactor. *Chin. Phys. C* **2013**, *37*, 58–62.
13. Zhang, L.G.; Shang, R.C. Analysis of influence of decay-cooling time on on-line burnup measurement of HTR-PM. *Nucl. Eng. Des.* **2009**, *30*, 43–46.
14. Hawari, A.I.; Chen, J.; Su, B.; Zhao, Z. Assessment of on-line burnup monitoring of pebble bed reactor fuel using passive gamma-ray spectrometry. In Proceedings of the 2001 IEEE Nuclear Science Symposium Conference Record, San Diego, CA, USA, 4–10 November 2001.
15. Lieder, R.M.; Jäger, H.; Neskakis, A.; Venkova, T.; Michel, C. Design of a bismuth germanate anti-Compton spectrometer and its use in nuclear spectroscopy. *Nucl. Instrum. Methods Phys. Res.* **1984**, *220*, 363–370. [[CrossRef](#)]
16. Badran, H.M.; Sharshar, T. An experimental method for the optimization of anti-Compton spectrometer. *Nucl. Instrum. Methods Phys. Res.* **1999**, *435*, 423–432. [[CrossRef](#)]
17. Kantele, J.; Marttila, O.J.; Hattula, J. Gamma spectrometer systems employing an anti-compton annulus. *Nucl. Instrum. Methods* **1966**, *39*, 194–216. [[CrossRef](#)]
18. Bomboni, E.; Cerullo, N.; Fridman, E.; Lomonaco, G.; Shwageraus, E. Comparison among MCNP-based depletion codes applied to burnup calculations of pebble-bed HTR lattices. *Nucl. Eng. Des.* **2010**, *240*, 918–924. [[CrossRef](#)]
19. Cerullo, N.; Bufalino, D.; Forasassi, G.; Lomonaco, G.; Rocchi, P.; Romanello, V. An additional performance of HTRS: The waste radiotoxicity minimisation. *Radiat. Prot. Dosim.* **2005**, *115*, 122–125. [[CrossRef](#)] [[PubMed](#)]
20. Xia, B.; Li, F.; Wu, Z. Burn-Up Calibration and Error Analysis of HTR-10 Spherical Fuel Elements by Gamma Spectroscopy. In Proceedings of the International Conference on Nuclear Engineering, Xi'an, China, 17–21 May 2010; pp. 437–444.
21. Xia, B. The Preliminary Simulation on the Physical Features in the Running-In Phase of the HTR-10. Ph.D. Thesis, Tsinghua University, Beijing, China, 2010.
22. Agostinelli, S.; Allison, J.; Amako, K.A.; Apostolakis, J.; Araujo, H.; Arce, P.; Asai, M.; Axen, D.; Banerjee, S.; Barrand, G.; et al. Geant4-A simulation toolkit. *Nucl. Instrum. Methods Phys. Res. A* **2003**, *506*, 250–303. [[CrossRef](#)]
23. Bender, S.E.; Ünlü, K.; Orton, C.R.; Schwantes, J.M. Geant4 model validation of Compton suppressed system for process monitoring of spent fuel. *J. Radioanal. Nucl. Chem.* **2013**, *296*, 647–654. [[CrossRef](#)]
24. Ionică, R.; Căta-Danil, G. Efficiency evaluation of a high resolution, low background gamma spectrometer with GEANT4. *UPB Sci. Bull.* **2008**, *70*, 75–82.

25. Tsutsumi, M.; Oishi, T.; Kinouchi, N.; Sakamoto, R.; Yoshida, M. Design of an Anti-Compton Spectrometer for Low-Level Radioactive Wastes using Monte Carlo Techniques. *J. Nucl. Sci. Technol.* **2002**, *39*, 957–963. [[CrossRef](#)]
26. *IEEE Standard Test Procedures for Germanium Gamma-Ray Detectors*; Ansi/IEEE Std.; IEEE: Piscataway, NJ, USA, 2002; pp. 1–32.



© 2018 by the authors. Licensee MDPI, Basel, Switzerland. This article is an open access article distributed under the terms and conditions of the Creative Commons Attribution (CC BY) license (<http://creativecommons.org/licenses/by/4.0/>).